Non- destructive characterization of carbon fiber composite/Cu joints for nuclear fusion applications

Valentina Casalegno[a], Milena Salvo, Monica Ferraris, Federico Smeacetto, Mario Merola*, Matteo Bettuzzi°
Materials Science and Chemical Engineering Department- Politecnico di Torino
C.so Duca degli Abruzzi,24- I- 10129, Torino, Italy
* ITER Organisation, Cadarache Centre, Bat 524, F-13108 Saint Paul lez Durance , France
°Physics Department, University of Bologna and INFN, Bologna, Italy

Abstract

Several non-destructive testing methods, lock-in thermography, ultrasonic inspection, microtomography and microradiography, were used to assess the manufacturing quality of joints between carbon fiber reinforced carbon composites and Cu/ CuCrZr.

The results revealed that ultrasonic inspection is critical since carbon composites and copper have a significant difference in the acoustic impedance; moreover this technique is sensitive to irregular shaped joined surfaces; microtomography and microradiography offer qualitative information on the joint, since carbon is significantly less X-rays sensitive than copper. Lock-in thermography gives information on thermal continuity at interface. Non destructive test results have been validated by destructive tests (morphological analysis and mechanical testing).

[a]Corresponding Author: Valentina Casalegno
Politecnico di Torino, Materials Science and Chemical Engineering Department,
Corso Duca degli Abruzzi 24-10129 TORINO, ITALY,
phone +39 011 564 4706
fax +39 011 564 4699,
valentina.casalegno @polito.it

1. Introduction

This paper introduces a qualitative approach for non-destructive tests and their evaluation for carbon fiber reinforced carbon composites and Cu-Cu alloys joints.

Reliable non-destructive tests (NDT) are fundamental for the manufacturing of components for nuclear fusion applications, especially for high heat flux plasma facing components.

NDT allow inspection of a component without impairing serviceability; it's important to detect and characterize defects (type, size and position) as well as the set-up of acceptance standards in order to predict their influence on the component performance in service conditions. NDT on carbon fibre reinforced carbon matrix composites/Cu joint are complex because of the different behavior of carbon fibre reinforced carbon matrix composites (CFC) and copper with regard to physical excitations used to test the component; furthermore the response to this input must be accurately assessed to identify the detachment of CFC tiles from Cu alloy.

The joints were developed for the high heat flux components of fusion machines: CFC/Cu tiles for flat-type armour and CFC/Cu/Cu-alloy brazed tiles for flat-type armour.

Joined samples were tested by NDT to evaluate the suitability of these tests on the joining technique proposed by the authors [1].

NDT includes various techniques, which allow inspection of a component without impairing serviceability. In effect, it's important to detect and characterize defects (type, size and position) in order to predict their influence on the component performance in service conditions. In CFC/Cu joints, the NDT target is to identify two different kinds of defects: detached interfaces or porosities in the cast copper.

Several studies have been dedicated to non-destructive investigation of the CFC/Cu joints, since these joints are one of the most critical issues in the high heat flux components [2-4].

The following techniques have been used in this work:

- Lock-in thermography
- Ultrasonic inspections

- Microtomography
- Microradiography

After NDT, metallographic investigation and mechanical tests were performed on the same samples to validate the NDT. The results of different NDT and their experimental validation will be discussed in this paper.

2. Materials and experimental procedure

The specimens used in the present investigation were CFC/Cu and CFC/Cu/CuCrZr joints. The carbon-carbon composites used were manufactured by Snecma Propulsion Solide; they are CFC NB31 and have a 3-D fibre perform made of ex-PAN and ex-pitch carbon fibres filled with a carbon matrix [5].

The copper used for CFC/Cu joints is Oxygen Free High Conductive copper (OFHC)., (Goodfellow) as a foil with thickness of 3.15 mm. The purity of copper was 99.95%. CuCrZr alloy (ITER grade) was produced by Kabel Metal.

The composite blocks were sliced into 22x19x8 mm pieces; cast copper was 2 mm thick and CuCrZr alloy brazed to CFC/Cu joint was 1-1.5 mm thick

The joints have been obtained using a process that modifies the surface of the composite and then cast copper on the modified surface, according to the procedure described in ref [1, 6, 7]. Chromium was used as metallizing modifier on the composite surface in order to react with C and form a carbide wettable by molten copper [8].The Cu/CuCrZr joints were obtained using a brazing filler (Gemco®). Gemco is a commercial alloy, produced by Wesgo Metals with the following composition: 87.75% Cu, 0.25% Ni, 12.00% Ge, %wt. The braze foil thickness is about 0.06 mm.

Samples and NDT are summarized in table 1.

Samples K,L and M were obtained by Cr modification of CFC surface and casting of copper was performed with external pressure of about 1 kPa. Samples D and E were achieved with CFC modified by Cr and casting of copper was performed under gas pressure (Ar overpressure =3 bar). Samples referred to as K, L and M were subjected to thermal fatigue test. The thermal fatigue tests on the joined samples were performed by heating the samples up to 450°C in air , followed by fast cooling from 450 to 25°C (in air with water quench, cooling rate = 60 °C/s). The cycles were repeated 50 times. Thermocouple put inside the sample, close to CFC/Cu interface allowed to record temperatures during test.

Samples L and M have a mechanical structuring of the CFC surface [1].

Samples referred to as D and E were not subjected to thermal fatigue tests and they were tested as prepared.

Ultrasonic inspection was carried out on samples K,L,M at Ansaldo Ricerche, Genova (Italy) and on samples K, L, D and E at Enea Casaccia , Rome (Italy), in order to compare two different ultrasonic set-ups.

The ultrasonic results are presented in different ways in figures 2-6: A-, B-,C-scan. A-scan gives the defect depth, its size and the nature through the signal amplitude; when the transducer is moved in a straight line on the surface of the sample under test, a series of A-scans can be recorded as a function of position; it's possible to obtain a representation of the cross-section of the sample normal to the surface and on the line of the scan. B-scan gives information on the depth in which the defect is located; C-scan gives a map of the attenuation level at different positions; it gives the spatial location in the plane of the sheet, but not the depth location, of any defect [9,10,11] .

The chosen ultrasonic frequency varies from 4 to 20 MHz; tests at Ansaldo Ricerche were performed using 10 MHz, while tests at ENEA were performed varying from 4 to 20 MHz (Karl-Deutsch TS6PB4-20P30 probe, crystal diameter 6 mm).. In each case, the transducer was placed on the CuCrZr or Cu side, since ultrasounds can hardly propagate inside the CFC material [12,13]. In order to get efficient ultrasonic waves propagation between the transducer and the joint, water was used as coupling medium to assure good acoustic coupling.

Sample M was tested using X-ray microtomography at University of Bologna (Italy) (experimental apparatus X-Ray CCD System (XCCD System) .

Sample K and L were tested by means of X-ray micro-radiography at NILPRP- Bucharest (Romania).

Lock-in thermography tests were performed on samples K and L. This technique, also known as photothermal thermography, has been set up in CEA/DRFC- Cadarache (France) [14, 15].

It is based on the study of thermal wave propagation into the examined sample due to an external sinusoidal thermal stimulation with an infrared device. A specific software records the response of the sample; the calculated phase-shift depends on the thermal diffusivity along the heat path, thus on the presence of flaws into the component.

Cross-sections of all the joined samples were analyzed by optical microscopy (REICHERT-JUNG MEF-3 metallographic optical microscope) and by scanning electron microscope (525M, JEOL JSM5200 and LEO 1450) .

Mechanical tests (single-lap shear test) were performed on the joined samples after NDT. The shear strength of the joints was measured at room temperature with a compression machine (SINTEC D/10), according to method described in ref [16]; the shear test configuration was adapted from ASTM D905 [17].

3. Results and discussion

As the ultrasonic waves travel through a material, they are modified by the material itself and by the presence of defects; at a boundary between two materials (i.e. CFC and Cu) a part of waves is reflected and the rest transmitted.

Any sound from the pulsed beam of ultrasounds that returns to the transducer like an echo is shown on a screen which gives the amplitude of the pulse and the time taken to return to the transducer. Defects anywhere through the specimen thickness reflect the sound, back to the transducer. If pores, voids, or defects exist at the joint interface, the reflection becomes stronger or dominant. Attenuation increases can indicate the presence of detachment between CFC and Cu or increased void content (presence of porosities at interface).

The transducer was designed to locate the focus point of the ultrasonic pulse at the joint interface. If the joint interface is continuous, the ultrasonic pulse emitted from the transducer can be transferred from the metallic material (Cu-CuCrZr) into the CFC tile with negligible reflection at the joint interface. If some defects exist at the joint interface, a reflection is recorded and then mapped according to the coordinates of ultrasonic scanning.

Figure 1 shows C-scans of each sample. Concerning sample K, it is possible to notice a significant echo (any sound from pulse that returns to the transducer) which means that defects through the specimen thickness reflect the sound, back to the transducer. White zones probably indicate a detached interface. A-scan in suspected detached region point out large echo and several reflected echoes; green/blue areas signify good joint interface.

With reference to sample L, one can note that, as for sample K, detected defects are located in the lower region of the samples, probably at interface CFC/Cu (yellow-red areas). Further tests (not reported here) showed an echo most likely due to Cu/CuCrZr interface that hides partly CFC/Cu interface. C-scan of sample M shows possible large defects at interface CFC/Cu, while only lower region (green area) looks not detached.

Ultrasonic inspection on samples K and L was also performed at ENEA-Casaccia. The focus was adjusted between CFC/Cu and Cu/CuCrZr interfaces, in order to have the same amplitude for echo signals : at 1 mm (it is the thickness of the CuCrZr alloy)and at 3-3.5 mm (it’s the total thickness of pure copper and CuCrZr alloy); signal amplification was constant (50 on A-scan color scale).The echo at Cu/water interface was considered as a reference for discontinuity (defect) both for CFC/Cu interface and Cu/CuCrZr interface.

The transducer was placed on the CuCrZr side.

At times the echo at the Cu alloy/water interface (signal from the top of the sample in contact with transducer to the interface takes 0.63µs since v=4.7 mm/µs and the distance top-cu/CuCrZr interface is 1.5 mm) and the second signal (distance top-Cu/CFC interface is 3 mm and then signal takes 1.3 µs) have the same amplitude. These conditions indicate a defect at interface.

C-scan in area of sample K (figure 2) pointed out a defect at Cu/CuCrZr interface; defect sizes are limited (about 2 mm^2); B-scan corroborates defect localization (echo at Cu/CuCrZr interface hides echo at Cu/CFC interface).

As a comparison, C-scan of a defects free area is shown in figure 3; it can be distinguished the signal at Cu/CFC interface at 3.5mm (about 1.5µs in the B-scan).

C-scan reported in figure 4 was obtained with an extended window over 3,5 mm in depth. Defects are localized on the left and on the right side of the sample at CFC/Cu interface (red areas). Blue areas show good joint interface (no defects).

Concerning test on sample L, reference signals have been determined as for sample K (about 1 mm Cu/CuCrZr interface and about 3 mm Cu/CFC interface that correspond to 0.43 µs and 1.3 µs on time axis respectively). Figure 5 shows discontinuities at CFC/Cu interface. Cu/CuCrZr interface is quite continuous; only limited area (figure 6) indicates a defect.

To sum up, ultrasonic inspection detected one small defect at the Cu/CuCrZr interface and large defects at the Cu/CFC interface both for sample L and for sample K,prepared with external pressure of about 1 kPa. Data from ENEA are comparable to results obtained from Ansaldo Ricerche investigation, in terms of localization of the defects. Ansaldo Ricerche analysis indicates more extended defects than ENEA analysis; this is due to differences in set up arrangement. It can be concluded that defects make up 50% and 40% of the interface for samples K and L, respectively. Joined samples L and M were manufactured after mechanical machining of the CFC surface, which results in a irregular shape of the joint interface. According to some authors [13], irregular shapes add complexity to ultrasonic testing . Indeed, an irregular joint surface can diffuse ultrasonic echos in all the directions.

Samples D and E were produced by copper direct casting on chromium carbide modified CFC under Ar overpressure (about 3 bar). They were ultrasonic inspected at ENEA-Casaccia in Rome.

The focus was in copper layer at 2 mm from top surface.

Figure 7 shows a comparison between C- and D-scan for sample D ; if the cursor is directed on yellow area, signal amplitude is more than 20 (relative amplitude); if it's directed on blue area, signal amplitude is significantly lower (less than 10); sample E shows the same behavior.

Typically, good joints show low echo values (relative amplitude below 8, showed in blue). As a consequence, samples D and E seem to be acceptable only in areas corresponding to blue zones on C-scans; since most of the maps are yellow-green, it could be concluded that samples quality is low. On the contrary, red areas are not present on the maps thus indicating that Cu and CFC are not detached.

Actually, the samples quality appears to be poor; this is probably due to weak interface but it cannot be excluded that some porosities in cast Cu are localized at the interface between copper and CFC and they act as a void at interface.

Other attempts were also made to characterize the joint by T/R technique (transparency); they showed lack of transmission signal. This is the consequence of CFC porosity.

Sample M was analyzed by X-ray micro tomography technique.

Tomography is a modification of conventional radiography. In computed tomography a flat fan-shaped or conical shaped beam of X-rays penetrates a thin slice of the sample under test and the intensity of the transmitted beam is recorded as a function of position across the beam to give an absorption profile of the transmitted beam. Computer analysis of the absorption profiles enables a cross-sectional image of the sample to be constructed through reconstruction algorithm.

In figures 8 and 9 are shown some tomography of sample M achieved with 85 kV peak energy with 0.8 mm Cu filter and 45 kV without filter respectively. In the first one, the copper layer is clearly observable, where the copper “finger-like” pattern at CFC/Cu interface can be distinguished , while in the second one, the CFC structure is more evident.

Since the CFC volume analyzed is significantly larger than copper, but has lower absorption (the linear absorption coefficient is lower), the attenuation distribution should be considered.

The effects of highly absorbing materials on tomographic reconstruction could lead to some “star-artifacts” (white rays radiating away from a spot, a typical star-like pattern also known as metal-artifact.) on the surface of the analyzed sample; they correspond to “lack of information” zones (figure 10). These spots could be explained as voids at CFC/Cu interface but actually they are reconstruction artifacts.

In order to avoid these artifacts, X-ray energy should be enhanced; nevertheless, there will be a lack of information on CFC bulk, since it’s less absorbent. In this case, the X-ray beam can penetrate the CFC bulk but there is not enough contrast to detect the CFC/Cu interface.

It’s very hard to detect defects at CFC/Cu interfaces with this kind of tomography, since carbon-carbon composites and copper have different X-ray behavior (CFC is significantly less X-ray sensitive than copper). Furthermore the application of this technique to large series production appears prohibitive from a cost and time standpoint.

X-ray micro-radiography was performed on K and L CFC/Cu/CuCrZr samples; the X-ray inspection focused on an area of 19x22 mm^2.

X-ray micro-radiography along the 19 mm side of the examined area (figure 11) shows the interface between CFC and copper; the structure suggests that molten Cu penetrates into CFC substrate in a “finger-like” pattern.

Figure 12 shows a tomographic reconstruction of the interface region, where CFC was intentionally removed by image processing; the “finger-like” penetration of Cu in CFC bulk is outlined.

Lock-in thermography tests were performed on samples K and L at CEA/DRFC- Cadarache (France); the test set up is described elsewhere [14]. The study of thermal wave propagation into the sample is based on the thermal diffusivity along the heat path; the presence of flaws into the component have influence on thermal comeback.

Phase contrast cartography was measured for samples K and L (figure 13); these phase contrast values are in the experimental noise.

The reduced heat transfer capability of some areas of the joined samples, in particular due to the presence of flaws at the interface CFC/Cu can be detected by this technique; not bonded areas indicated by non-homogeneity of the values of the phase contrast cannot be detected in figure 13. As a consequence no defects on K and L samples were detected by means of this technique, in contrast with results of ultrasonic tests.

Samples K and L (prepared with 1 kPa, L also with mechanical structuring of the CFC surface) were submitted to mechanical tests after thermal fatigue tests, in order to evaluate the shear strength of the examined joints and to connect mechanical strength to the supposed defects in the samples. Samples failed at about 20 MPa; these values are lower than those obtained for samples not submitted to thermal fatigue tests (average shear strength≈ 33 MPa, [6] but still comparable to the interlaminar shear strength of the CFC NB31 (15MPa) [5].

The decrease in shear strength of samples K and L can be due to cracks generated during thermal fatigue stress or to the presence of pre-existing defects.

Average shear strength measured on more than 50 samples (joining process was performed with external pressure of about 1 kPa ,the same process as for K and L) is about 33 MPa, regardless of a range of porosity (from some µm to some mm) in cast copper or at CFC/Cu interface was observed in the samples' cross-sections or at the fracture surfaces. Therefore, the lower shear strength of samples K and L are due to thermal stresses induced during thermal fatigue. Defects seem to have little influence on mechanical strength of the joint in comparison with thermo-mechanical stress induced by thermal fatigue testing.

Shear strength of sample D and E was 25 MPa; these sample were manufactured without external pressure during copper casting but using Ar overpressure, and they were not submitted to thermal fatigue test.

Ultrasonic inspection gave divergent results also for examination of CFC NS31 (silicon doped carbon-carbon) joined to Cu; 5 samples were tested before thermal fatigue test. Sample 1 and 5 (figure 14) showed many defects, especially sample 5 in the upper part (yellow area); these two samples sustained 30 cycles during thermal fatigue test and fracture surface analysis didn't reveal significant detached areas at interface.

Metallographic inspection was performed on each sample after NDT. The samples were cross-sectioned along directions where flaws were supposed to be.

On sample M (prepared with 1 kPa, after thermal fatigue tests and mechanical structuring of the CFC surface) the morphological analysis revealed that no defects were present in the sample, in contrast to results from the ultrasonic tests. Both optical microscopy and SEM analysis of cross sections of the joint (reported in figure 15 a) showed that the interfaces are not detached and there are no voids or cracks in the joint; detected defects by ultrasonic analysis in sample M are not confirmed by morphological inspection.

With regard to samples D and E (prepared with Ar overpressure, not subjected to thermal fatigue tests, tested as prepared) optical analysis of cross sections of the joints (figures 15 b,c,d) shows detached interfaces along some direction where defects were supposed to be, while CFC/Cu interface is continuous in some areas of the joint where the NDT saw large defects.

Results of metallographic inspection on samples D and E agree partially with ultrasonic inspection that foresaw a weak adhesion between CFC and copper; the CFC/Cu interface is partly detached. Conversely, some areas indicated as discontinuous by US analysis look sound (figure 15 b).

SEM and optical micrographs on samples K and L (figure 16) revealed some voids at CFC/Cu interface, but at the same time supposed detached areas are not confirmed by morphological inspection; as a consequence metallographic analysis doesn't agree completely with results from ultrasonic inspection and ultrasonic analysis disagrees with lock-in thermography.

It can be explained if discontinuities at CFC/Cu interface are small (reduced gap between CFC and Cu surfaces). In that sense, the thermography map can't point out discontinuity at the interface, since thermal response of the joint is quite good; on the contrary mechanical strength should be low.

In table 2 a summary of discussed results is reported.

Defect free samples, validated by NDT, morphological analysis and mechanical tests are not available yet.

4. Conclusions

The results of non-destructive characterization of CFC/Cu-Cu alloy joints have been presented. Based on the results of the tests on several samples, the following conclusion can be drawn:

- Reliability of non destructive tests of joints should be validated by destructive tests such as morphological evidence of the detected defect and mechanical testing.
- ultrasonic inspection on CFC/Cu joints gave unreliable results; this can be explained considering that CFC and copper have a significant difference in the acoustic impedance; therefore high ultrasonic echo exists even if the joint is good; as a consequence defects in the CuCrZr/Cu brazed joints can be identified, but those at the CFC/Cu joint interface can hardly be detected. Another disadvantage of ultrasonic inspection is that it is sensitive to irregular shaped (e.g. mechanically structured) joined surfaces.
- X-ray tomography can only offer a qualitative information on CFC/Cu interface, since carbon is significantly less X-rays sensitive than copper
- Lock-in thermography offers information on thermal continuity at interface and can predict the component behavior under critical heat flux event, since it gives a global information about the soundness of the heat path, but not necessarily on the chemical continuity at the interface; the advantage of Lock-in thermography is that it is not sensitive to irregular shaped jointed surfaces and it can be also used for machined CFC/Cu joint.

- Shear tests (e.g. single-lap) are reliable in detecting defects in the joint: unfortunately, it is a destructive test, but, together with microscopy, it should be used to validate each proposed NDT.

Acknowledgements

The authors are grateful to Dr. F. Escourbiac (CEA) for lock-in thermography analysis, to Dr. R. Vesprini (ENEA) and to Dr.C.Ozzano (Ansaldo Ricerche) for ultrasonic investigation; thanks to AnsaldoRicerche (Dr. M.Grattarola) for supplying materials.

References

[1] Appendino P,Casalegno V, Ferraris M, Grattarola M, Merola M, Salvo M. Direct Joining of CFC to Copper. Journal of Nuclear Materials. 329-333 (2004) 1563-1566.

[2] Merola M, Chappuis P, Escourbiac F, Grattarola M, Jeskanen H, Kauppinen P, et al. Zabernig. Non-destructive testing of divertor components. Fusion Engineering and Design. 61-62 (2002) 141-146.

[3] Ezato K, Dairaku M, Taniguchi M, Sato K, Akiba M. Non-destructive testing of CFC monoblock divertor mock-ups. Journal of Nuclear Materials. 307–311 (2002) 144–148.

[4] Escourbiac F, Constans S, Courtois X, Durocher A. Application of lock-in thermography non destructive technique to CFC armoured plasma facing components. Journal of Nuclear Materials. 367–370 (2007) 1492–1496.

[5] Merola M, Wu C H and the EU ITER Participating Team, Development of carbon materials and plasma facing components for ITER. Physica Scripta. T111 (2004) 152–156.

[6] Appendino P, Ferraris M, Casalegno V, Salvo M, Merola M, Grattarola M. Proposal for a new technique to join CFC composites to copper. Journal of Nuclear Materials 348 (2006) 102-107.

[7] Ferraris M, Casalegno V, Salvo M. Process to join carbon based materials to metals and its applications. International Patent WO2005037734, (2005).

[8] Eustathopoulos N, Nicholas M.G., Drevet B. Wettability at high temperature. Pergamon Ed., 1999, chapter 3 and 8.

[9] Krautkrämer J, Krautkrämer H. Ultrasonic testing of materials. Berlin Sprinter, 1990, pp. 27-55.

[10] Associazione Italiana di metallurgia. Le prove non distruttive vol.1. Centro prove non distruttive,1984, p 395.

[11] Kar A., Palit Sagar S., Kumar Ray A., Characterization of the ceramic–metal brazed interface using ultrasonic technique . Materials Letters 61 (2007) 4169–4172

[12] Durocher A., Schlosser J., Cordier J.J., Agarici G. Quality control of plasma facing components for Tore Supra. Fusion Engineering and design 66–68 (2003) 305.

[13] Merola M, Akiba M, Barabash V, Mazul I. Overview on fabrication and joining of plasma facing and high heat flux materials for ITER. Journal of Nuclear Materials 307–311 (2002),1524–1532.

[14] Escourbiac F, Constans S, Courtois X, Durocher A. Application of lock-in thermography non destructive technique to CFC armoured plasma facing components. Proceedings of ICFRM 12, Santa Barbara (USA), 2005; 45-49.

[15] Wu D., Zweschper Th., Salerno A., Busse G., Lock-in Thermography for Nondestructive Evaluation of Aerospace Structures, NDT.net (1998) Vol.3 No.9

[16] Ferraris M, Salvo M, Isola C, Appendino Montorsi M, Kohyama A. Glass-ceramic joining and coating of SiC/SiC for fusion applications. Journal of Nuclear Materials 258–263 (1998),1546-1550.

[17] ASTM D905– 98, “Standard Test Method for Strength Properties of Adhesive Bonds in Shear by Compression Loading”.

Captions

Figure 1 C-scan of a CFC NB31/Cu/CuCrZr joined sample

Figure 2   Defect at Cu/CuCrZr interface in sample K

Figure 3 Maps of ultrasonic investigation on sample K; defect free CuCrZr/Cu interface gets observable CFC/Cu interface

Figure 4 Defects localization (red color on the C-scan) at Cu/CFC interface for sample K

Figure 5 CFC/Cu interface scan of sample L : defects are located in yellow-red areas

Figure 6 Defect at Cu/CuCrZr interface (yellow/red dot in blue area)in sample L

Figure 7 C-scan (on the left) of sample D; the probe was pointed on the yellow area marked by the cross of yellow lines; D-scan on the right

Figure 8 Images from tomography of sample M; CFC bulk is not shown; the interface between CFC and copper can be detected

Figure 9 Cross-sectional image of M sample achieved by tomography; it can be noticed the CFC bulk where are clearly observable CFC fibers

Figure 10 Artifacts at the CFC/Cu interface

Figure 11 X-ray micro-radiography along the 19 mm side of the tested sample K

Figure 12 Image reconstructed from tomography analysis of CFC/Cu interface

Figure 13 phase contrast cartography for samples A and B

Figure 14 Ultrasonic map on 5 CFC NS31 (silicon doped)/Cu joined samples

Figure 15 a) SEM magnification of CFC/Cr carbide/Cu interface of sample M; b) Optical micrograph showing defect-free cross section of sample D; on the right, it is possible to identify a pore in the carbon matrix; c) Optical micrograph of sample D showing detached interface between CFC and copper on the right, d) Image from optical microscopy characterization of sample E: there is a significant detach at CFC/Cu interface (about 600 μm)

Figure 16 SEM magnification of cross-sections of samples K and L: both for sample L and for sample K some areas at CFC/Cu interface are not continuous while some others don’t show any detached interface

Table 1 - NDT and analyzed samples: samples K, L and M were obtained with Cr modification of CFC surface and joining process was performed with external pressure of about 1 kPa. Samples D and E were realized with CFC modified by Cr and casting of copper was performed under Ar overpressure; Samples L and M have a mechanical structuring of the CFC surface.

*= Samples subjected to thermal fatigue test; samples referred to as D and E were not subjected to thermal fatigue tests and they were tested as prepared

Table 2 Summary of NDT results (Yes and No means “defect detected” and “no defect detected” respectively); joining process was performed with external pressure of about 1 kPa for sample K, L and M; casting of copper was performed under Ar overpressure for samples D and E. Samples L and M have a mechanical structuring of the CFC surface. Samples * were submitted to thermal fatigue test

[1] morphological analysis was performed on cross-section of the samples where defects were supposed to be; sometimes defect presence was observed (Yes), while in other case no defects were detected (No).Samples were cross-sectioned along several directions in order to investigate large areas

Figure 1

K

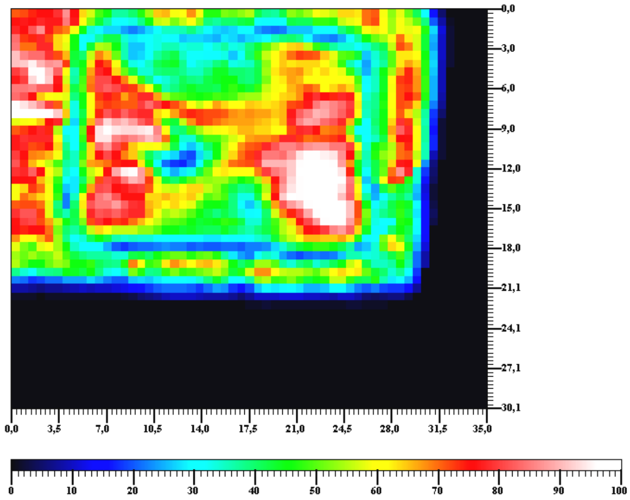
0,0 3,5 7,0 10,5 14,0 17,5 21,0 24,5 28,0 31,5 35,0
0,0 -3,0 -6,0 -9,0 -12,0 -15,0 -18,0 -21,1 -24,1 -27,1 -30,1
0 10 20 30 40 50 60 70 80 90 100

L

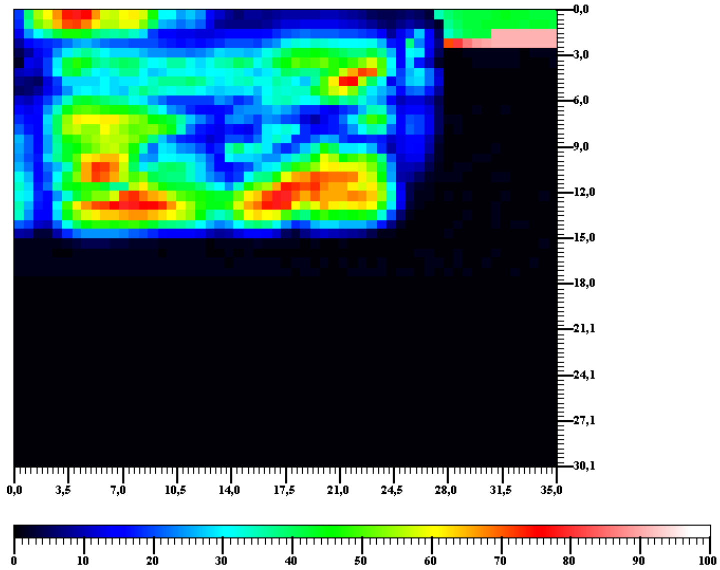
0,0 3,5 7,0 10,5 14,0 17,5 21,0 24,5 28,0 31,5 35,0
0,0 -3,0 -6,0 -9,0 -12,0 -15,0 -18,0 -21,1 -24,1 -27,1 -30,1
0 10 20 30 40 50 60 70 80 90 100

M

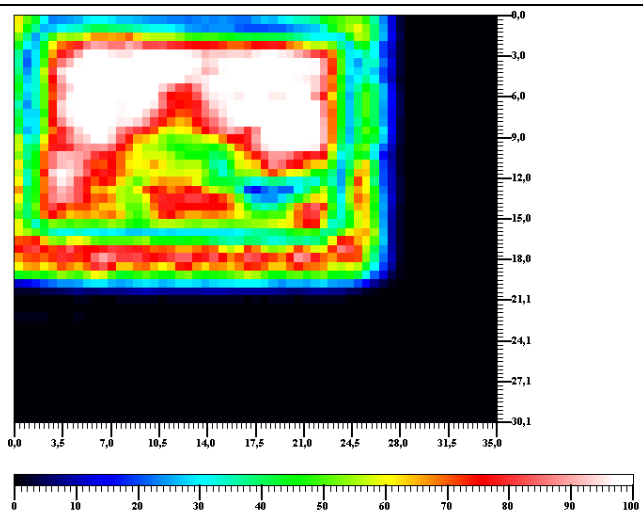
0,0 3,5 7,0 10,5 14,0 17,5 21,0 24,5 28,0 31,5 35,0
0,0 -3,0 -6,0 -9,0 -12,0 -15,0 -18,0 -21,1 -24,1 -27,1 -30,1
0 10 20 30 40 50 60 70 80 90 100

Figure 2

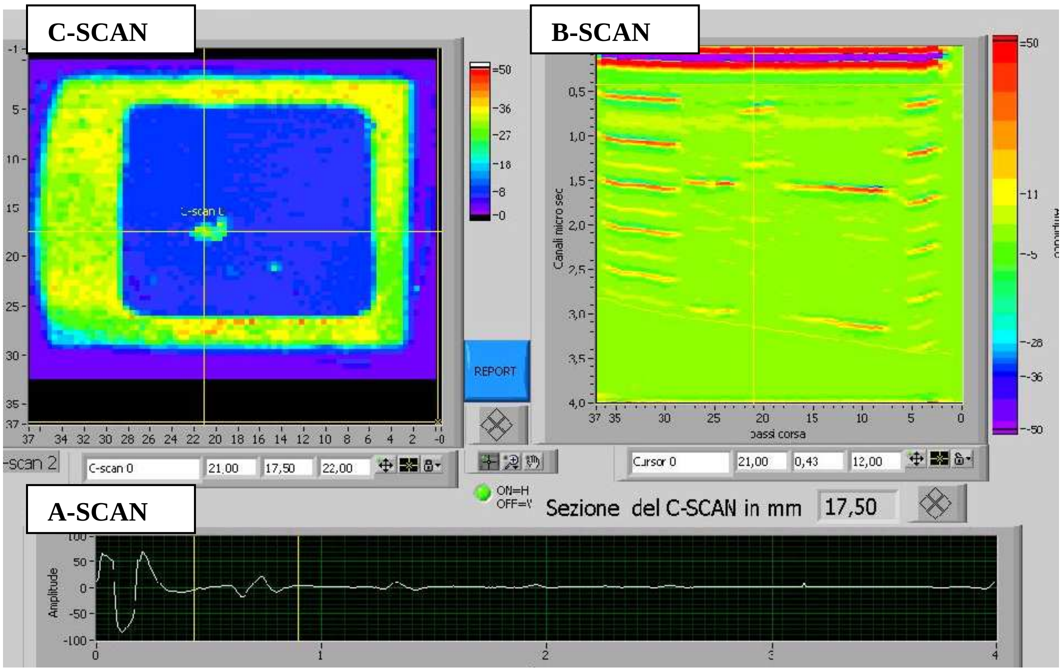

Figure 3

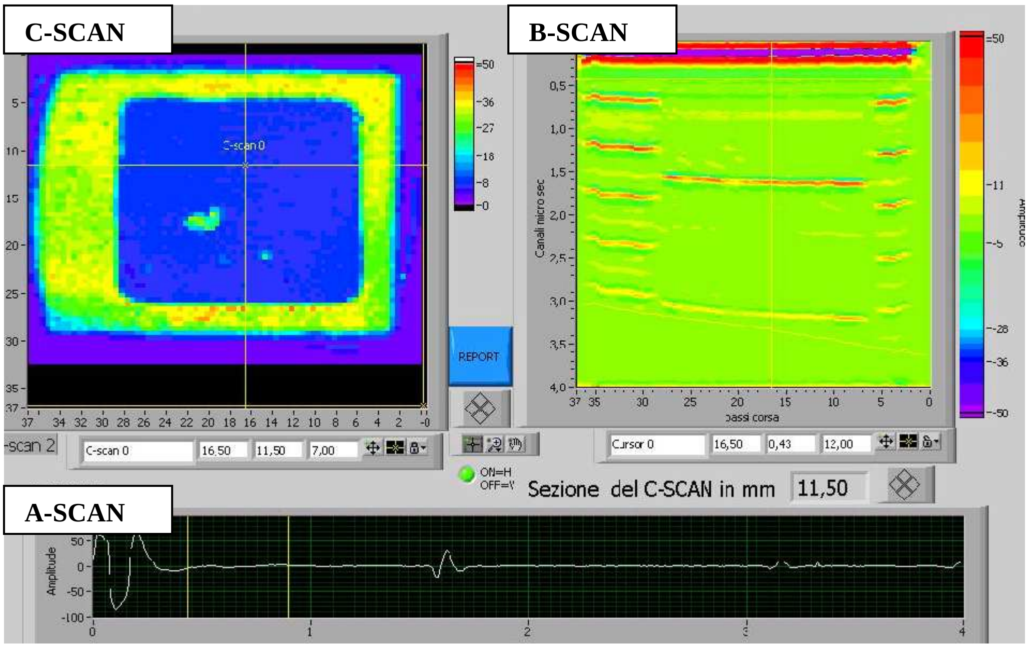

Figure 4

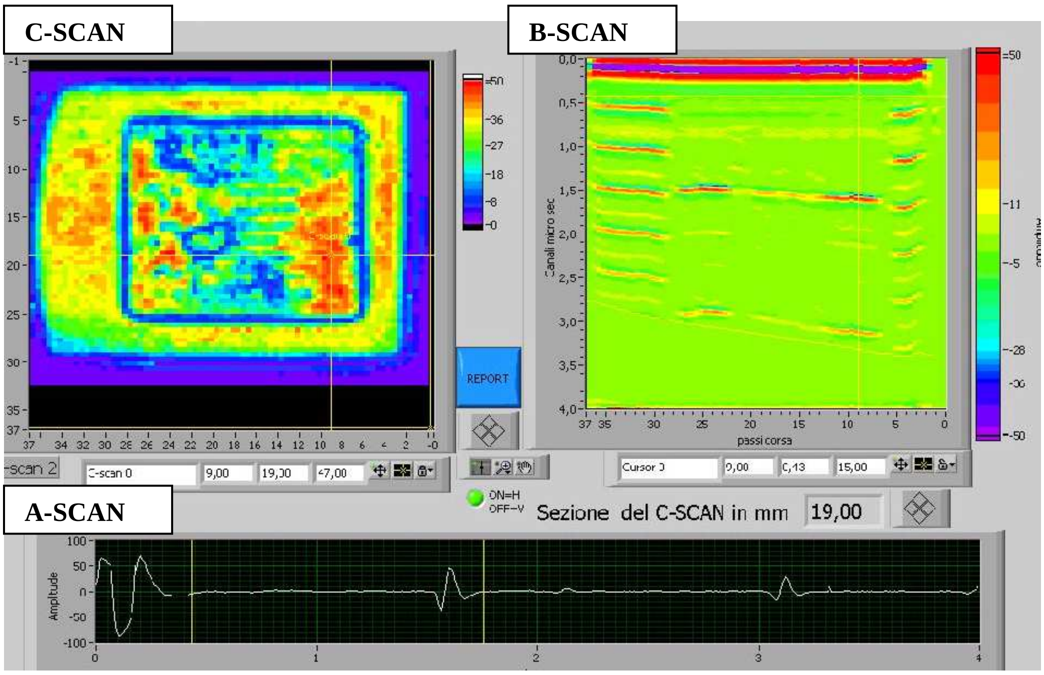

Figure 5

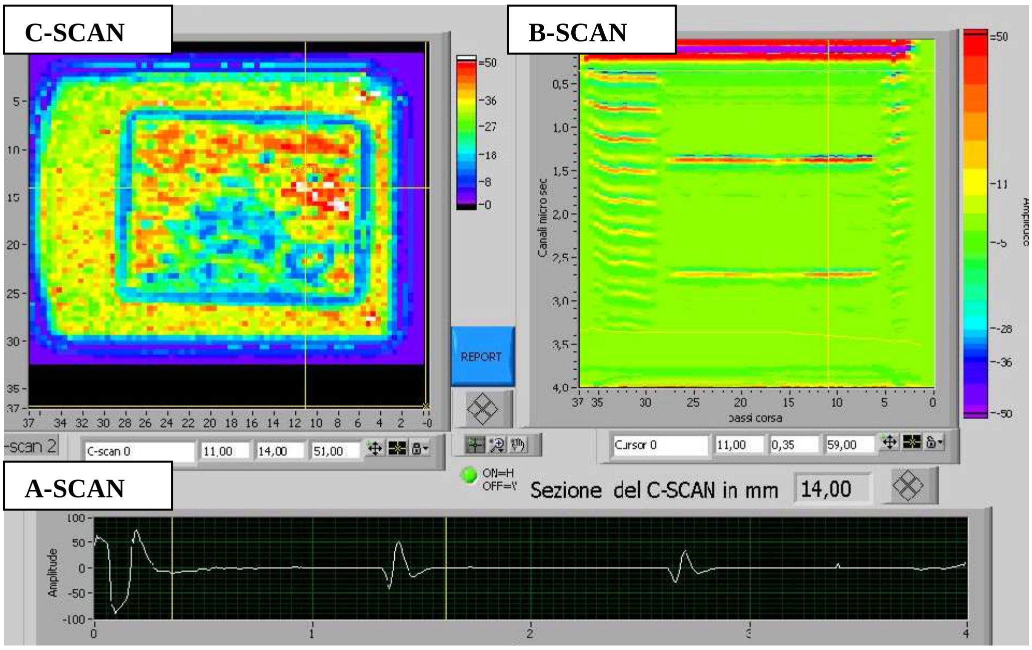

Figure 6

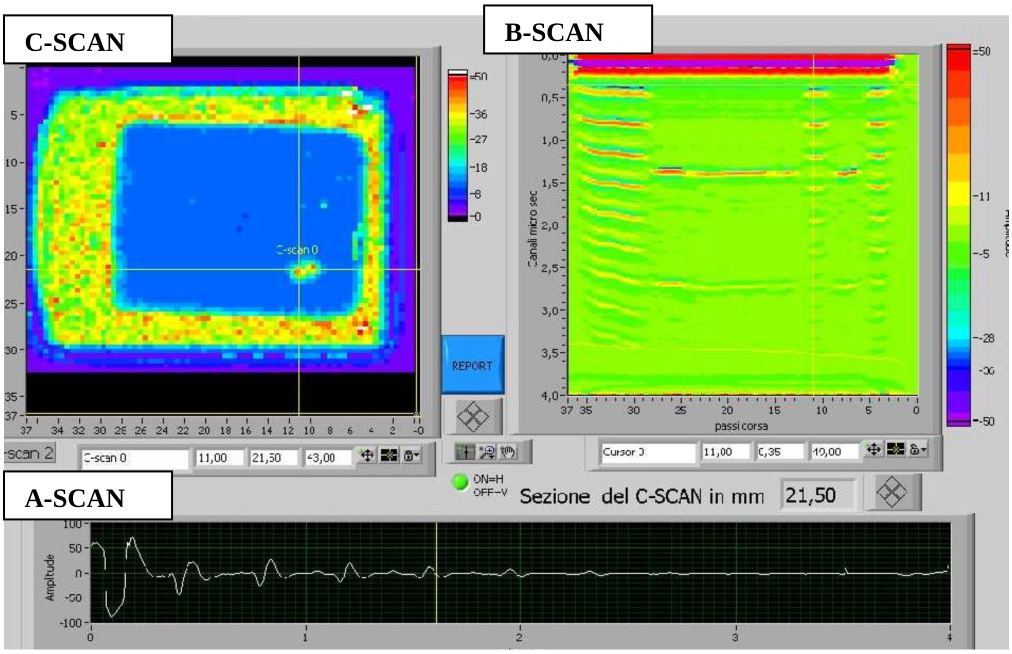

Figure 7

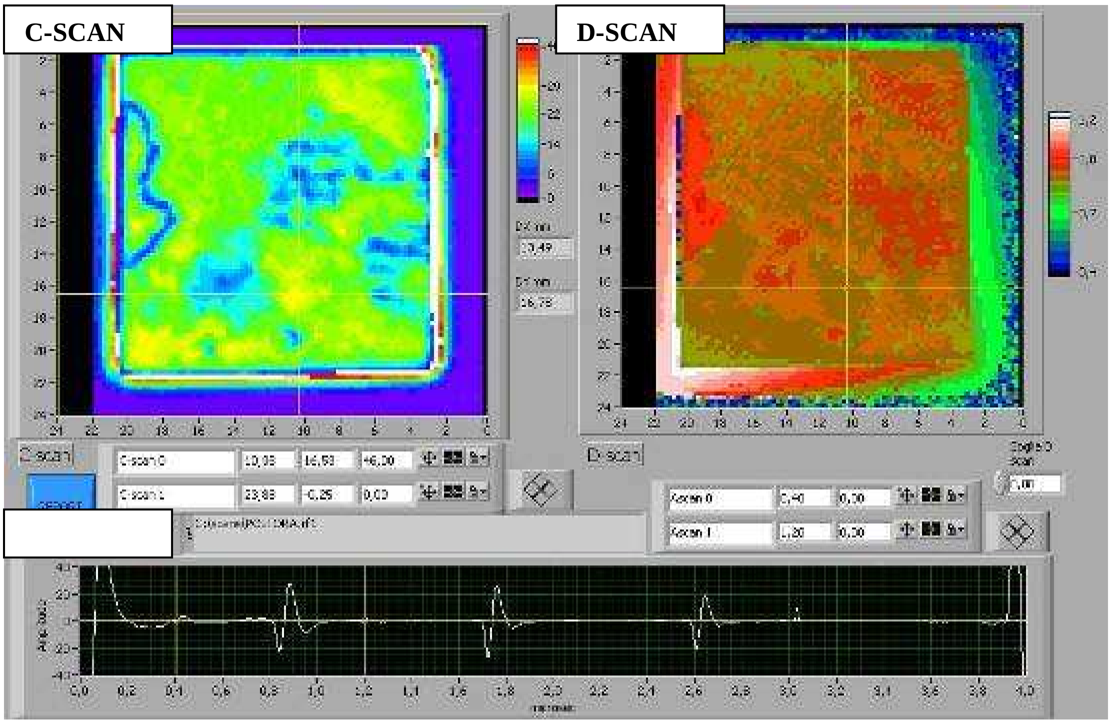

Figure 8

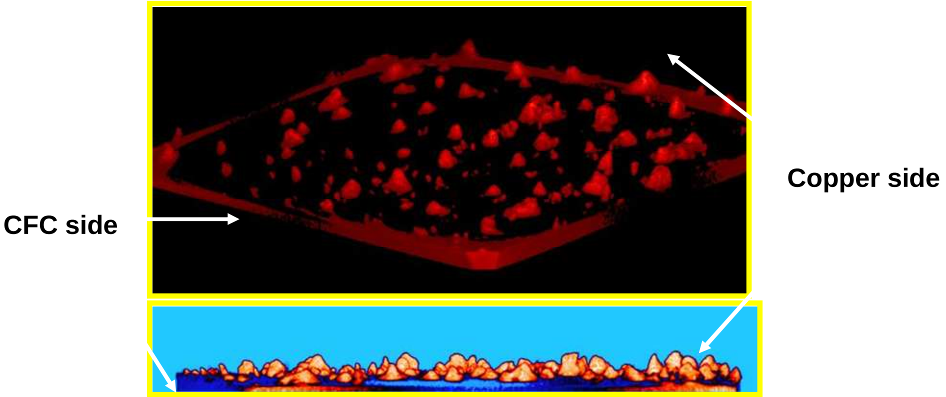

Figure 9

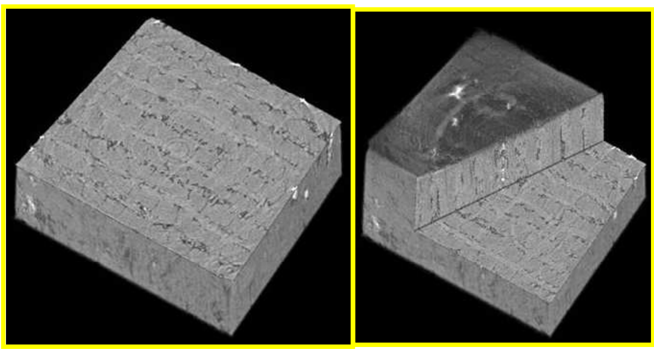

Figure 10

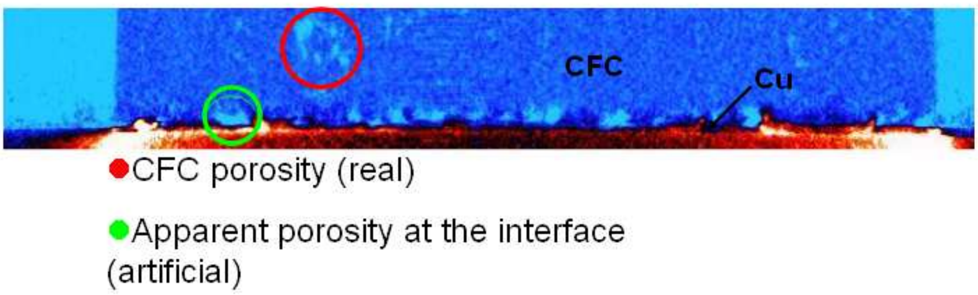

Figure 11

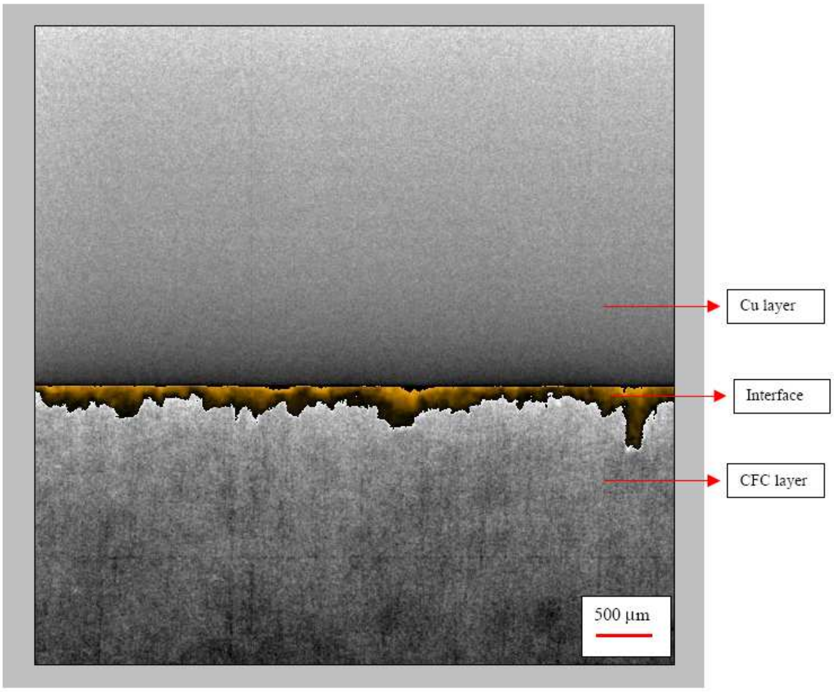

Figure 12

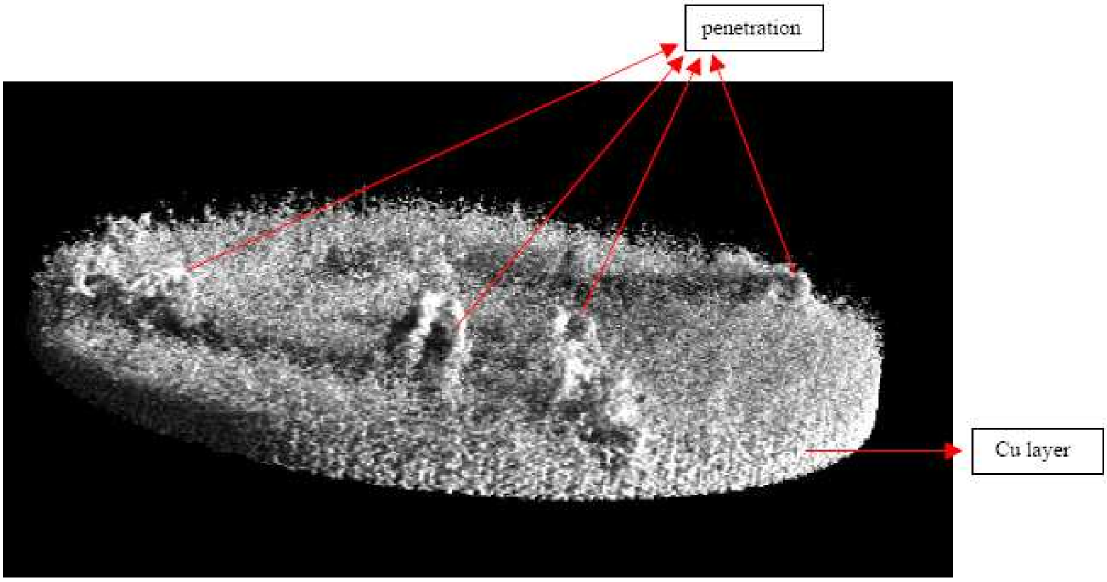

Figure 13

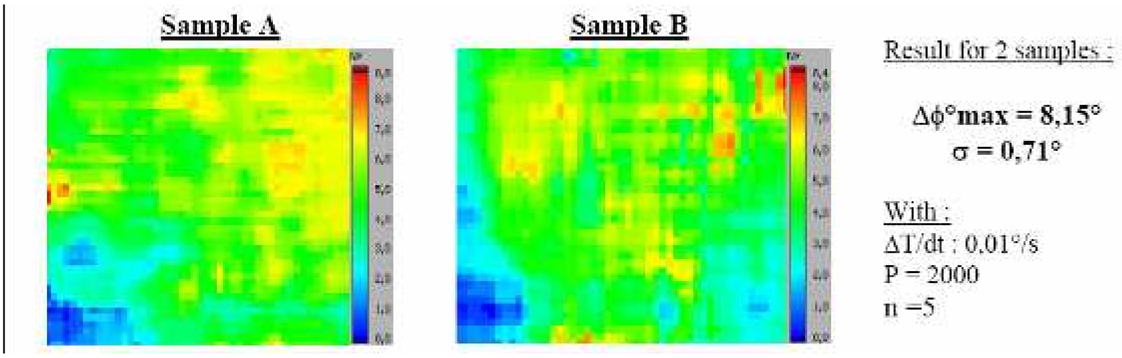

Figure 14

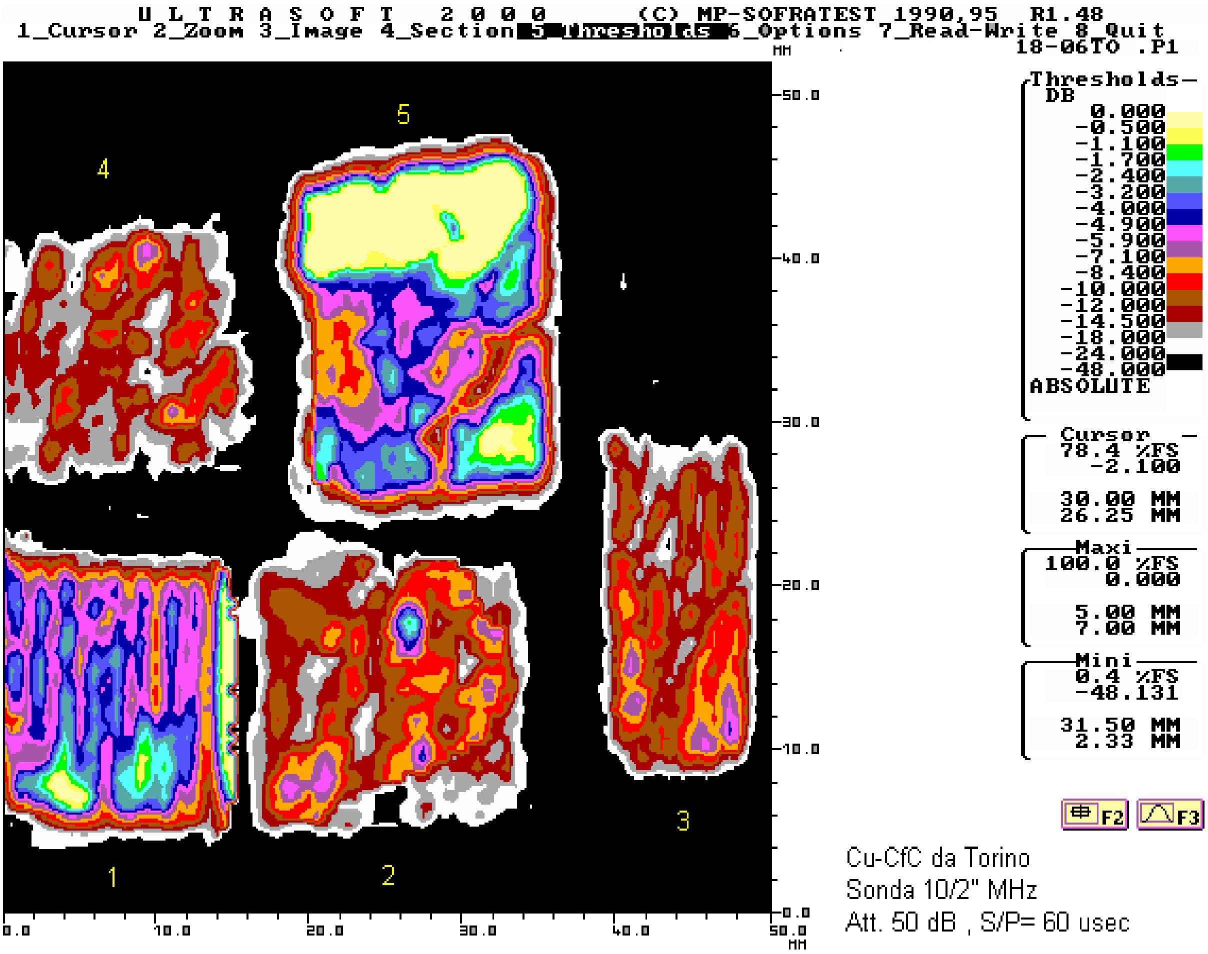

Figure 15

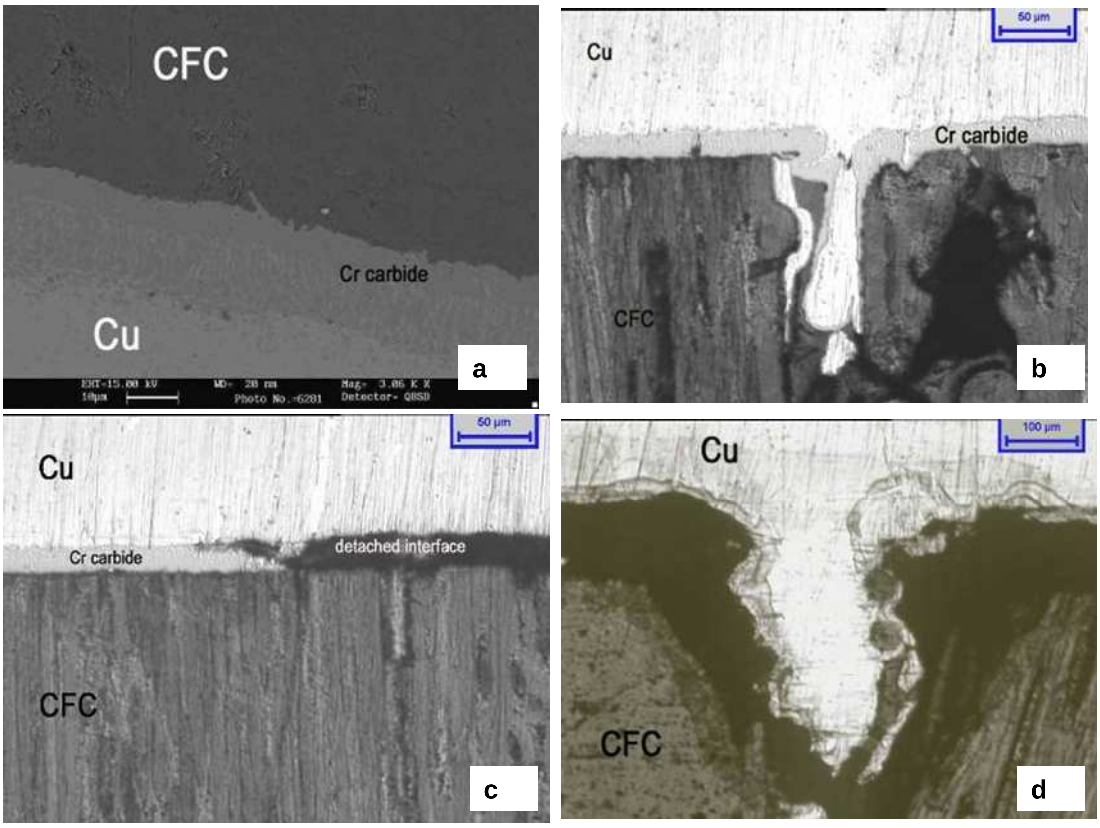

Figure 16

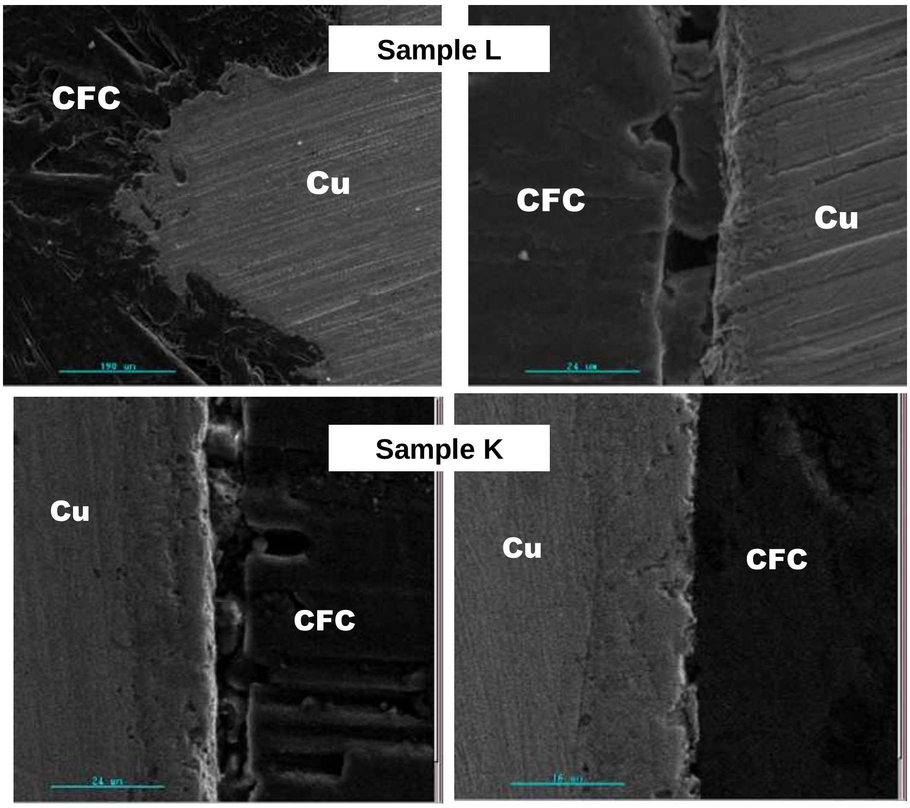

Table 1

		NON DESTRUCTIVE TEST						
SAMPLE	**JOINT AND MANUFACTURING TECHONOLGY**	**ULTRASONIC INSPECTION (Ansaldo Ricerche)**	**ULTRASONIC INSPECTION (ENEA)**	**LOCK-IN THERMO-GRAPHY**	**TOMOGRAPHY**	**X-RAY MICRORADIOGRAPHY**	**MORPHOLOGICAL INVESTIGATION**	**MECHANICAL TEST (SINGLE-LAP SHEAR TEST)**
K	CFC NB31/Cu/CuCrZr *	✓	✓	✓		✓	✓	✓
L	machined CFC NB31 /Cu/CuCrZr *	✓	✓	✓		✓	✓	✓
M	machined CFC NB31 /Cu/CuCrZr *	✓			✓		✓	
D	CFC NB31/Cu		✓				✓	✓
E	CFC NB31/Cu		✓				✓	✓

Table 2

	Defects detection by different NDTs (Yes/No)						
sample	**Ultrasonic inspection (Ansaldo)**	**Ultrasonic inspection (ENEA)**	**Lock-in Thermography**	**X-Ray micro radiography**	**Tomography**	**SEM/Optical microscopy**	**Shear strength [MPa]**
K*	Yes	Yes	No	No	-	Yes/No[1]	20
L*	Yes	Yes	No	No	-	Yes/No[1]	21
M*	Yes	-	-	-	Not suitable	No	-
D		Yes				Yes/No[1]	26
E		Yes				Yes /No[1]	26